Iranian Journal of Chemical Engineering
Vol. 15, No. 4 (Autumn 2018), IAChE

Optimization of Solvothermally Synthesized ZIF-67 Metal Organic Framework and Its Application for Cr (VI) Adsorption from Aqueous Solution

N. Mostafazadeh, A. A. Ghoreyshi [*], K. Pirzadeh

Chemical Engineering Department, Babol Noshirvani University of Technology, Babol, Iran

ARTICLE INFO

Article history:
Received: 2018-06-20
Accepted: 2018-09-22

Keywords:
Adsorption,
Cr (VI),
ZIF-67,
Solvothermal,
Regeneration

ABSTRACT

In this study, ZIF-67 was synthesized through solvothermal method to remove Cr (VI) ions from aqueous solution. To improve the structural properties of ZIF-67 and its adsorption capacity, optimization of the synthesis conditions was carried out based on maximum Cr (VI) uptake. From experiments, the optimum condition comprised solvent: metal ion molar ratio of 4.6:1, ligand: metal ion molar ratio of 318:1, and temperature of 23 ℃. The physio-chemical properties of as-synthesized ZIF-67 were investigated by BET, XRD, FTIR, and FESEM analyses. Effects of adsorption pH, adsorbent dosage, initial concentration, and contact time on adsorption process were investigated. Based on the results, the maximum adsorption capacity of Cr (VI) was 26.27 mg/g which was obtained at 35 ℃, pH of 5, adsorbent dosage of 3 g/l, and initial concentration of 107.82 mg/l. The equilibrium time for Cr (VI) adsorption varied from 180 min for low initial concentration of 9 mg/L to 240 min for a high initial concentration of 90 mg/L. For the synthesized ZIF-67, maximum uptake capacity was reported 26.27 mg/g at the initial concentration of 107.82 mg/l. The equilibrium data were described by Langmuir-Freundlich isotherm model better than the other models at three different temperatures. Pseudo-second-order model fitted the experimental data better than pseudo-first-order one. Adsorption thermodynamics indicated that the adsorption process was endothermic and spontaneous in nature. The regenerability of ZIF-67 was also studied in three sequential cycles, and the Cr (VI) adsorption was almost retained after two cycles.

1. Introduction

Over the last few decades, the amount of various pollutants in surface water and groundwater resources has increased due to the rapid development in industries and urbanization. As a consequence, the environment and the ecosystem have been polluted by excessive discharge of contaminants, especially heavy metals. Separation of these pollutants from the aquatic medium is one of the most important issues in the world [1]. Chromium is one of

[*]Corresponding author: aa_ghoreyshi@nit.ac.ir

the most hazardous heavy metals that can be found in wastewaters and has the highest destructive effect on the environment due to its high water solubility and toxicity [1, 2]. There are numerous industries that produce a large amount of chromium such as electroplating, leather tanning, dyeing, metal processing, and artificial fertilizers [2, 3].

The most stable forms of chromium in nature are Cr(III) and Cr (VI) in which Cr (VI) is more toxic than Cr(III) [4]. Long-term exposure to Cr (VI) may bring about several obstacles and illness to human beings such as vomiting, nausea, epigastric pain accompanied by the digestive tract, and lung cancer [5-7]. According to the United States Environmental Protection Agency (US EPA) and World Health Organization (WHO), the maximum permissible levels of Cr (VI) in drinking water are around 0.1 mg/l and 0.05 mg/l, respectively [8].

There are various techniques (i.e., physical, chemical, and biological methods) for removing Cr (VI) from aqueous solutions and wastewaters such as chemical precipitation, coagulation, biological operations, membrane filtration, and adsorption [8-14]. However, high operation costs, long operation time, large amount of sludge, and toxic by-product productions are some restrictions of these approaches [15]. Adsorption is a physio-chemical technique that is preferred to other methods because of its high efficiency, cost-effectiveness, and ease of operation characteristics [16]. So far, various porous materials, such as activated carbons, carbon nanotubes, zeolites, and chitosan, have been used as adsorbents for adsorption of Cr (VI) from aqueous solution [11].

Metal organic frameworks (MOFs) are a new class of porous crystalline organic-inorganic hybrid compounds constructed from metal clusters or ions and organic linkers. MOFs have emerged as interesting materials for various applications including energy storage [17], adsorption/separation [18], CO_2 adsorption [19], catalysis [20], luminescence [21], sensor [22], magnetism [23], and drug delivery [24]. These types of adsorbents attracted much attention due to their large surface areas, permanent porosity, and tunable pore properties [25-27]. Various methods have been proposed for MOF synthesis including solvothermal [28], hydrothermal [29], microwave-assisted [30], sonochemical [31], electrochemical [32], and mechanochemical [33]. Among these techniques, the solvothermal or hydrothermal route is the most commonly reported one in the synthesis of MOFs. The main reason that the solvothermal method is preferred to other techniques is the implementation of the synthesis process at atmospheric pressure and ambient temperature, which is associated with considerable energy saving. The MOF structure and characteristics can change by altering the synthesis parameters such as metal ion:ligand:solvent molar ratio, and synthesis temperature.

Zeolitic imidazolate frameworks (ZIFs) are a sub-family of MOFs in which tetrahedral metal ions (Co^{2+} or Zn^{2+}) are bridged by imidazolate ligands [34]. In addition, the structures of ZIFs have close similarity to aluminosilicate zeolites; hence, ZIFs benefit from the properties of both zeolites and MOFs [35, 36] such as high surface areas, high crystallinities, exceptional thermal and chemical stabilities [37], unimodal micropores, and abundant functionalities [35, 36, 38]. Several MOFs have been synthesized as an adsorbent for removing Cr (VI) ions from aqueous solution. For instance, in 2017, Niknam et al. employed ZIF-8 to remove Cr

(VI) from aqueous solution [39]. ZIF-8 was synthesized through the solvothermal method, and its specific surface area was 1281 $m^2.g^{-1}$. Their results indicated that ZIF-8 was unable to adsorb Cr (VI) ion from aqueous solution very well. In 2015, Li et al. used ZIF-67 for the removal of Cr (VI) from aqueous solution [8]. They reported that the adsorption capacities for initial concentrations of 6, 10, and 15 $mg.L^{-1}$ of Cr (VI) solution were 5.88, 9.32, and 13.34 $mg.g^{-1}$, respectively [8]. In review of the formation of ZIF particles by the solvothermal method, several researchers investigated the effect of various synthesis conditions such as metal ion:Hmim:MeOH molar ratios in the synthesis solution [40, 41], synthesis duration [42], solution pH [43], and temperature [44] on the characteristics of synthesized ZIF particles.

The main objective of this study is to synthesize ZIF-67 through the solvothermal method and its application for Cr (VI) ions removal from the aqueous solution. To improve the structural properties of ZIF-67 and, therefore, to enhance adsorption capacity, the synthesis conditions were optimized through variation in synthesis key parameters. Then, the optimum sample was characterized by several analyses, such as BET, FTIR, and FE-SEM, for a better understanding of ZIF-67 structure. The effect of operating parameters, that is, solution pH, adsorbent dosage, initial solution concentration, absorbent contact time, and temperature, was studied on Cr (VI) ion removal from aqueous solution by optimized ZIF-67. The equilibrium data were evaluated by different isotherm models, and the quickness of the adsorption process was interpreted by kinetic models. The adsorption thermodynamics was also studied to determine the adsorption nature. Finally, to assess the ZIF-67 uptake stability, three sequential adsorption-desorption processes were carried out.

2. Experimental

2.1. Materials

Cobalt nitrate hexahydrate, 2-methylimidazole, methanol, potassium dichromate, acetone, and 1,5 diphenylcarbazide (DPC) were of analytical grade and were purchased from Merck (Darmstadt, Germany).

2.2. Synthesis of ZIF-67

The ZIF-67 was synthesized through the solvothermal method based on a procedure reported by Jiang et al. [45]. In brief, 0.249 g cobalt nitrate hexahydrate was completely dissolved in 25 mL of methanol until forming a clear solution. In a separate beaker, 0.328 g 2-methylimidazole was dissolved in the same amount of methanol as it was used for metal salt. Afterwards, the prepared solutions were mixed and stirred at ambient temperature for 48 h to ensure the reaction was completed. Then, the resulting purple precipitates were centrifuged and washed three times with ethanol. Finally, ZIF-67 with purple color was dried overnight in the oven at 100 °C. For further experiments, the effects of Co^{2+}:Hmim (1:2 to 1:10) and Co^{2+}:MeOH (1:200 to 1:1444) molar ratio on the adsorption capacity of ZIF-67 were investigated.

2.3. Characterization

Crystallinity and solid phase structure of the as-synthesized ZIF-67 were studied by X-ray Diffraction (XRD) analysis (X pert Pro, Panalytical, Germany) using monochromatic Cu-Kα radiation (λ=1.5406 A°) with the current and voltage of 20 mA and 30 kV, respectively. The textural and microporous properties of ZIF-67 were determined by

nitrogen adsorption-desorption at 77K over the relative pressure range of 0.01-0.99 using Brunauer-Emmett-Teller (BET) surface area analyzer (BELSORP-mini II, Japan). The presence of surface functional groups was checked by Fourier Transform Infrared (FTIR) spectroscopy (TENSOR 27, Brucker, Germany) using KBr pellet in the range of 400–4000 cm^{-1}. To study surface morphology and microstructure of the ZIF-67, Field Emission Scanning Electron Microscope (FESEM, MIRA3TESCAN-XMU) analysis was implemented by Tescan instrument (MIRA3, Czech) with the acceleration voltage of 5 kV. For conductivity purposes and better observations, the samples were gold sputtered before the analysis.

2.4. Batch adsorption experiment

Adsorption experiments were carried out to determine the optimal conditions for the removal of Cr (VI) from aqueous solutions. Stock solution of Cr (VI) was prepared by dissolving an appropriate amount of $K_2Cr_2O_7$ in distilled water; for each experiment, desired concentrations were prepared by diluting the stock solution with distilled water. Batch adsorption experiments were conducted by adding an appropriate amount of ZIF-67 samples to 10 mL of Cr (VI) solutions with specified initial concentrations and a certain pH value and, then, placed in an incubator shaker (IKA KS 4000i, Germany) at 180 rpm at various operating temperatures. To study the adsorption kinetics, a certain amount of samples were taken at equal time intervals until the equilibrium reached. For this purpose, the adsorbent was separated from the aqueous solutions by means of a syringe filter (0.45 μm, poly tetra fluoro ethylene). The concentration of Cr (VI) ion in the solution was determined in an acidic solution with diphenylcarbazide at 540 nm by UV-Vis spectrophotometer (2100 SERIES, UNICO, USA). The effects of key parameters on Cr (VI) removal, such as pH (3-8), adsorbent dosage (1-5 g/L), and temperature (19, 25, and 35 ℃), were studied to obtain the optimal condition. The initial pH of the Cr (VI) solutions was adjusted with 0.1 M NaOH and 0.1 M HCl, respectively the optimal initial concentration was determined by adding an optimal dosage of adsorbent in 10 mL of Cr (VI) solution. The amount of Cr (VI) adsorbed per unit mass of the adsorbent can be determined by the mass balance equation:

$$q = \frac{V(C_0 - C_e)}{m} \quad (1)$$

where q (mg/g) is the amount of Cr (VI) adsorbed per gram of adsorbent, C_0 and C_e are the initial and equilibrium concentrations of Cr (VI) in the solution (mg/L), respectively, m is the mass of the adsorbent used (mg), and V (L) is the initial volume of the Cr (VI) solution.

The removal percentage of Cr (VI) ions by the ZIF-67 can be calculated by the following equation:

$$\%\,R = \frac{C_0 - C_e}{C_0} \times 100 \quad (2)$$

3. Results and discussion

3.1. Synthesis results

3.1.1. Effect of different Co^{2+}: MeOH molar ratios

Co^{2+}: MeOH molar ratio is one of the most influential parameters with a substantial effect on ZIF-67 structure and adsorption capability. In this regard, various ratios of metal salt to solvent, i.e., 1: 200, 1: 318, 1: 867, 1: 1000, 1: 1400, and 1: 1444, were selected to find the optimum condition that shows the highest Cr (VI) adsorption capacity. All samples were

synthesized in similar conditions in which 1 g/L of each sample was subjected to direct contact of Cr (VI) solution with an initial concentration of 50 mg/L at 298 K. The amount of Cr (VI) uptake by each sample is listed in Table 1. According to Table 1, it can be understood that as the Co^{2+}: MeOH molar ratio decreased from 1:1444 to 1:318, the adsorption capacity and removal efficiency of Cr (VI) increased from 33.2 mg/g to 40.15 mg/g and from 59.28 % to 72 %, respectively. This can be attributed to the fact that when the amount of MeOH in the solution decreases, the concentration of Co^{2+} ions and imidazolium increases in the medium leading to the formation of small-sized particles resulting from rapid nucleation and crystal growth stage [46-48]. As the Co^{2+}: MeOH molar ratio reduced from 1: 318 to 1: 200, the adsorption capacity and removal efficiency of Cr (VI) decreased from 40.15 mg/g to 23.75 mg/g and from 72 % to 45.24 %, respectively. Since the amount of cobalt salt and ligand was redundant as opposed to the volume of the solvent, the solution became saturated and no further dissolution could be observed. Therefore, an imbalance will occur in the stoichiometry of the reaction.

Table 1
The adsorption capacity and removal efficiency of ZIF-67 in Cr (VI) removal at different Co^{2+}: MeOH molar ratios.

Co^{2+}: MeOH	1:200	1:318	1:867	1:1000	1:1400	1:1444
% Removal	45.24	72	70.70	68	62.28	59.28
q_t (mg/g)	23.75	40.15	39.60	38	34.88	33.20

3.1.2. Effect of different Co^{2+}: Hmim molar ratio

When the optimum condition for Co^{2+}: MeOH molar ratio was determined, finding the best (optimum) Co^{2+}: Hmim molar ratio was the next target. For this purpose, different molar ratios of ligand to metal salt (1:2 to 1:10) were chosen. Based on these molar ratios, adsorption experiments were implemented at ambient temperature, the initial concentration of 50 mg/L, and adsorbent dosage of 1 g/L. The results (Cr (VI) uptake and removal percentage) are tabulated in Table 2. From Table 2, it can be understood that an increase in Co^{2+}: Hmim molar ratio up to 1:4.6 enhanced the adsorption capacity and Cr (VI) removal percentage about 37 mg/g and 76 %, respectively. This can be attributed to the fact that by raising the Co^{2+}: Hmim molar ratio, the crystal seeds would be surrounded by the excessive amount of ligands, limiting further connections between organic and inorganic sections. The consequence of this occurrence is the formation of smaller particles during crystal growth [48, 49]. However, a further increase in Co^{2+}: Hmim molar ratio up to 1:10 led to a reduction in adsorption capacity and removal efficiency of Cr (VI) from 37 mg/g and 76 % to 31 mg/g and 68 %, respectively, which may be due to the failure of the complete dissolution of 2-methylimidazole in methanol.

Table 2
The adsorption capacity and removal efficiency of Cr (VI) by as-synthesized ZIF-67 with different Co^{2+}: Hmim molar ratios.

Co^{2+}: Hmim	1:2	1:4.6	1:8	1:10
% Removal	50	76	69	68
q_t (mg/g)	23	37	32	31

3.1.3. Effect of temperature on the as-synthesized ZIF-67

The synthesis temperature is another parameter that can have a positive or negative effect on MOFs structure. For this purpose, ZIF-67 was synthesized at three temperatures of 23, 30, and 40 ℃; then, the ZIF-67 samples were used for adsorption of Cr (VI) from a solution with the initial concentration of 50 mg/L, adsorbent dosage of 1 g/L and temperature of 25 ℃. The outcomes from the adsorption process, i.e., adsorption capacity and removal efficiency, were calculated, as listed in Table 3. According to Table 3, it can be deduced that at 23 ˚C, ZIF-67 showed the maximum Cr (VI) uptake and removal percentage. This issue is also confirmed by BET analysis, as indicated in Table 3. The ZIF-67 synthesized at 23 ˚C possesses the highest specific surface area and pore volume among other samples. The main reason can be attributed to the high crystallinity of ZIF-67 at low temperature; on the other hand, there is a possibility of crystals aggregations at higher temperatures in which the crystal does not show a well-defined rhombic dodecahedral morphology [50-52].

Table 3
Textural properties of synthesized ZIF-67 and adsorption capacity and removal efficiency of Cr (VI) by ZIF-67 at different temperatures.

Temperatures (℃)	23	30	40
% Removal	72	57.27	47
q_t (mg/g)	40	32.35	26.52
Specific surface area (m^2/g)	1767.6	1744.8	1673.8
Total pore volume (cm^3/g)	0.6885	0.6769	0.6649

3.2. Characterization results

Based on the results obtained in the previous sections, the optimum condition for synthesizing ZIF-67 was determined, and the optimum sample was characterized by several analyses. The crystal structure of the as-synthesized ZIF-67 is shown in Fig. 1. As is depicted in Fig. 1, all diffraction peaks shown in this figure are identical to their corresponding simulated samples [46, 53]. This indicates that the structure of the ZIF-67 is well preserved and no more impurities are sighted. The sharp and strong diffraction peaks in Fig. 1 indicate the high crystallinity nature of the ZIF-67. The intensive peak at low 2θ=7.1° can be attributed to the (110) crystal plane of ZIF-67, which is much higher than other peaks, denoting a favorable orientation of the (110) crystal plane direction [8].

The surface morphology and the geometry of optimized ZIF-67 were studied by Field emission scanning electron microscopy (FE-SEM), as shown in Fig. 2. It is evident from the FE-SEM analysis that the adsorbent is composed of a large number of regular particles with uniform and perfect rhombic dodecahedral morphology [8].

Fig. 3 shows the FT-IR spectra of the ZIF-67 structure before and after the adsorption of Cr (VI) ions. The IR spectrum of the as-synthesized ZIF-67 was recorded in the range of 400–4,000 cm^{-1}. In the FTIR spectrum of the ZIF-67, the peak at 3128.42 and 2927.57 cm^{-1} shows the presence of the aromatic and aliphatic C–H stretch of the imidazole, respectively. The bands at 1639.84 and 1423.25 cm^{-1} are attributed to the stretching vibration of C=N group of the imidazole and C═C double bonds, respectively [54]. The

peak at 3438.13 cm^{-1} is assigned to stretching (O–H) vibration in hydroxyl groups, and the band at around 424.15 cm^{-1} is ascribed to Co–N stretch. After the adsorption process, the intensity of the peak at around 424.15 cm^{-1} decreased because of the reduction of the electron density of nitrogen and cobalt. This phenomenon occurs when nitrogen in the ligand structure donates electrons to cobalt ion. Then, the electrons are transferred to Cr (VI) ions, reducing them, to Cr(III) ones [8].

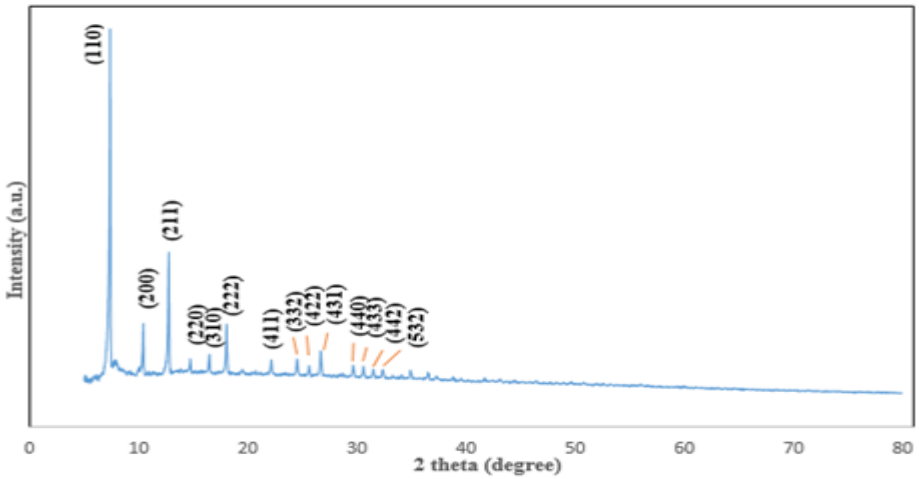

Figure 1. Experimental XRD patterns of as-synthesized ZIF-67.

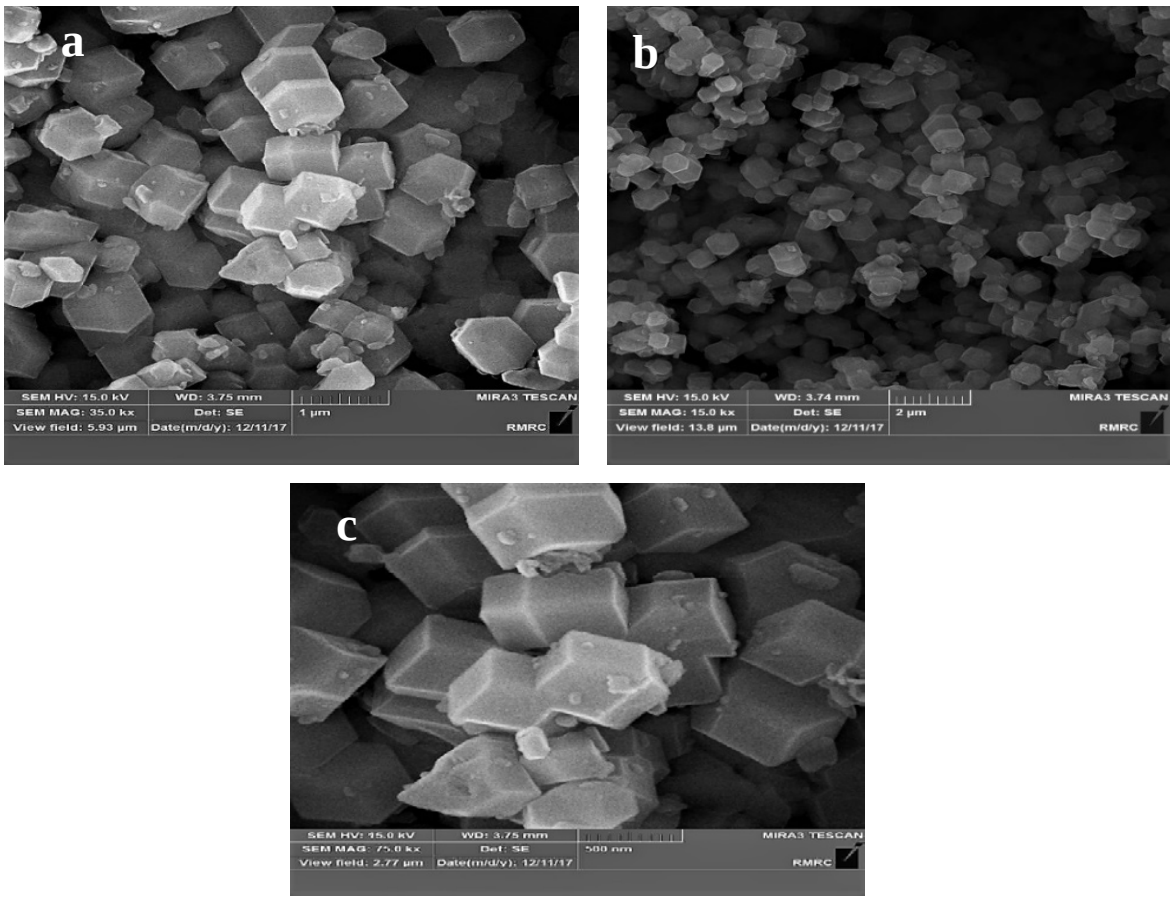

Figure 2. FE-SEM micrographs of ZIF-67 at different magnifications: (a) 1 µm, (b) 2 µm, and (c) 500 nm.

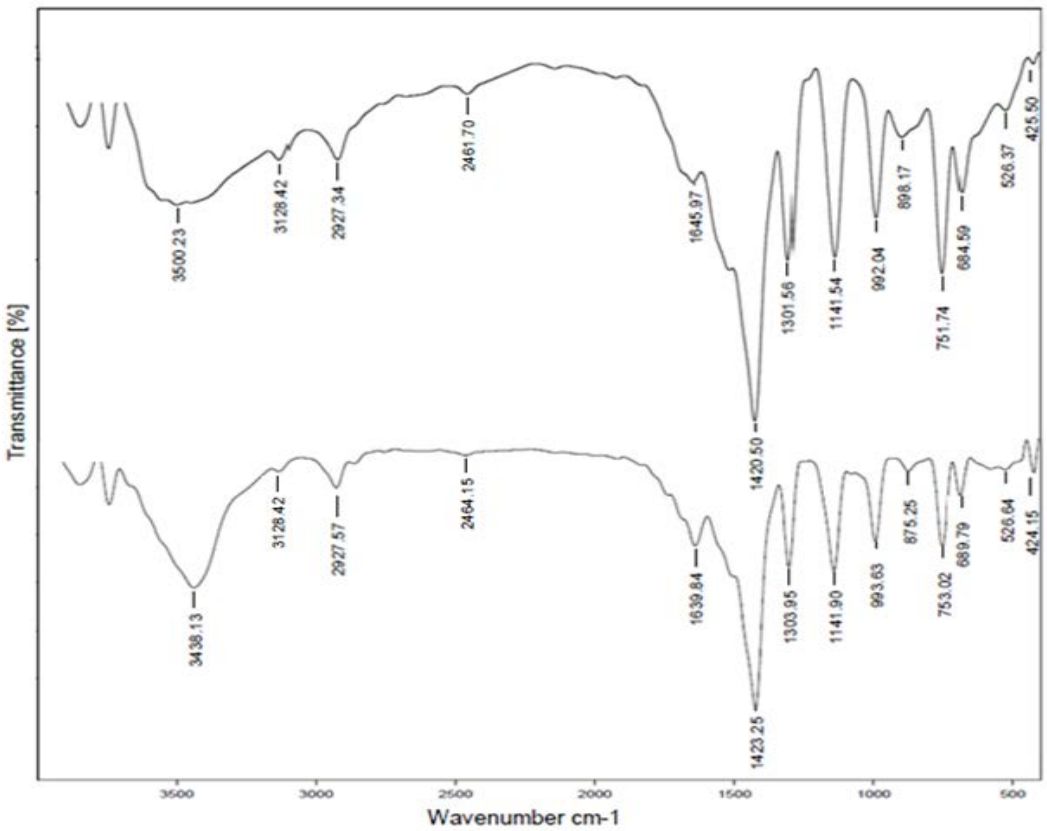

Figure 3. FT-IR spectra of the as-synthesized ZIF-67: (a) before adsorption of Cr (VI) and (b) after adsorption of Cr (VI).

The textural properties of the as-synthesized ZIF-67 were determined by N_2 adsorption-desorption experiment at 77 K, as illustrated in Fig. 4. The nitrogen adsorption-desorption isotherm trends followed type I isotherm according to IUPAC classification, corresponding to microporous solids. Fig. 5 shows the pore size distribution of the ZIF-67 microcrystals resulting from MP and BJH methods. As it is clear from Fig. 5a, the majority of pore sizes are below 1 nm, which are in accordance with Fig.4; thus, it is confirmed that the ZIF-67 has a highly microporous structure.

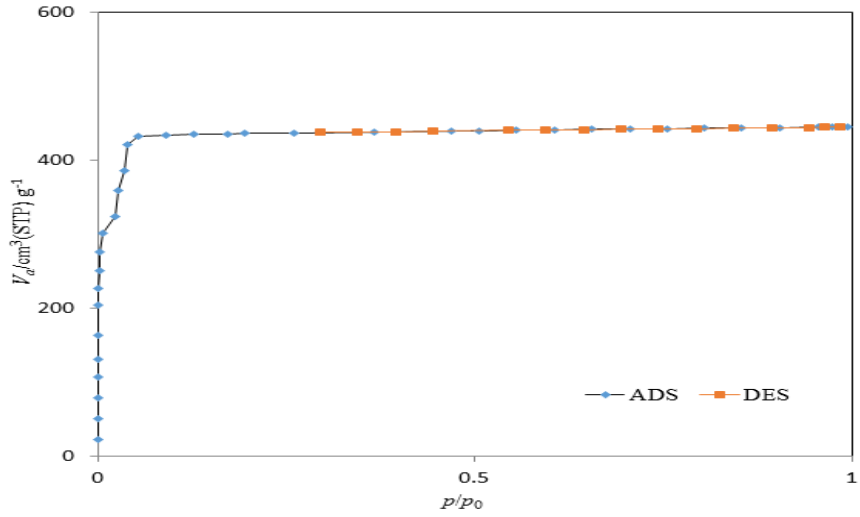

Figure 4. Adsorption/desorption isotherms of N_2 at 77 K on ZIF-67.

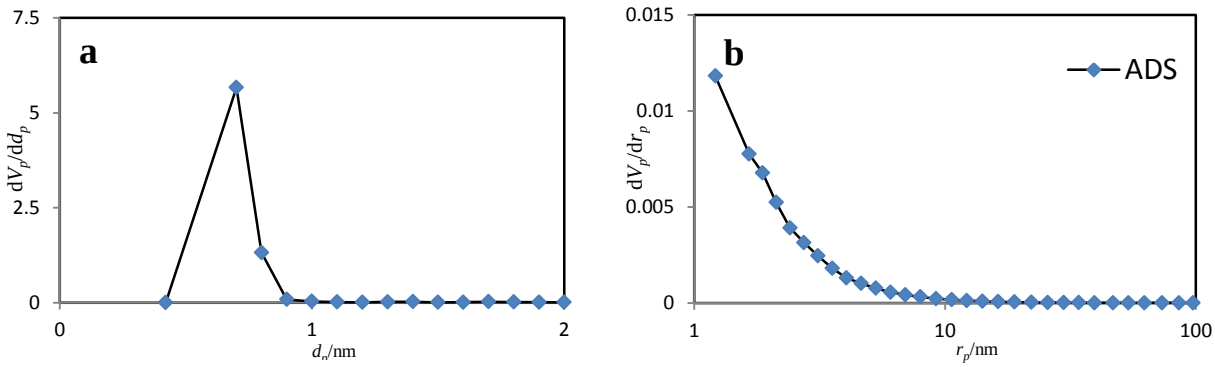

Figure 5. (a) MP (b) BJH plots of ZIF-67 MOF.

Detailed information about the ZIF-67 textural properties, including specific surface area, total pore volume, and micropore volume, is listed in Table 4.

Table 4
Textural properties of as-synthesized ZIF-67.

Sample	S_{BET} (m^2/g)	$V_{micropore}$ (cm^3/g)	$V_{mesopore}$ (cm^3/g)	V_{total} (cm^3/g)	Mean pore diameter (nm)
ZIF-67	1767.6	0.6868	0.0017	0.6885	1.5581

3.3. Adsorption results

3.3.1. Effect of pH on Cr (VI) adsorption

The solution pH is one of the most important parameters in the adsorption process, since it determines the surface charge of the adsorbent and the degree of ionization of the adsorbate [55, 56]. Cr (VI) ions can be found in various forms in aqueous solution at different pH values, such as H_2CrO_4 (pH<1.0), $HCrO_4^-$ and $Cr_2O_7^{2-}$ (pH 2.0-6.0), and CrO_4^{-2} (pH >6.0) [57]. ZIF-67 can effectively remove toxic Cr (VI) in two different ways: electrostatic interaction and ion exchange in which Cr (VI) partially reduces to less toxic Cr(III) ion [8]. The pH_{pzc} of ZIF-67 is around 8.7 [8]; therefore, ZIF-67 surface is positively charged when the pH is below 8.7 and electrostatically attracts negatively charged ions ($HCrO_4^-$, $Cr_2O_7^{2-}$, and $Cr_2O_7^{2-}$). To determine the optimum pH for Cr (VI) mitigation, the experiments were conducted in the pH range of 3-8, while temperature, contact time, initial concentration, and adsorbent dosage were kept unchanged at 298 K, 180 min, 50 mg/L, and 1 g/L, respectively. Fig. 6 illustrates the effect of pH on Cr (VI) adsorption. As can be seen from Fig. 6, there is a sharp increase in Cr (VI) removal when the pH of the solution raised from 3 to 5. This might be assigned to the reduction of H^+ ion concentration in the medium that comes into competition with $HCrO_4^-$, interacting with the positively charged surface of the adsorbent. A further increase in solution pH up to 8 brought about a decrease in Cr (VI) removal from 47.28 % to 29.51 %. This may be due to an increase in the concentration of hydroxyl ions on the ZIF-67 surface, enhancing a repulsive force between the negatively charged adsorbent surface and the CrO_4^{2-} ions. As pH increases, CrO_4^{2-} will be the dominant species of chromium ion in the solution that cause a reduction in ion exchange between hydroxyl groups and chromate ions since the ionic strength of chromate ions is weaker than that of the hydroxyl ions [58-60].

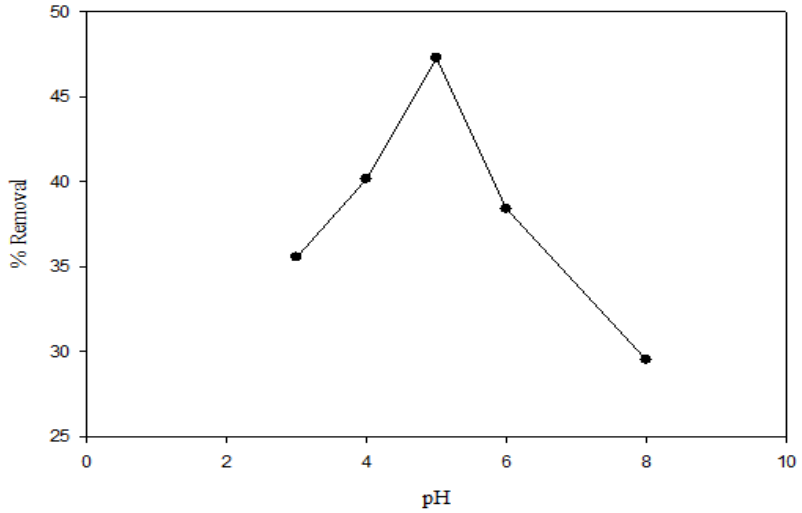

Figure 6. Effect of pH on Cr (VI) removal (T=298 K, C_0=53 mg/L, adsorbent dosage of 1 g/L).

3.3.2. Effect of adsorbent dosage on Cr (VI) removal

Adsorbent dosage is another important parameter in the adsorption process that determines treatment cost and the adsorbent capacity for a given adsorbate concentration [61]. To determine the optimal dosage of adsorbent, various amounts of ZIF-67 from 1-5 g/L were examined for 180 min at 25 ℃, pH of 5, and the initial concentration of 51 mg/L. The adsorbent dosage effects on adsorption capacity as well as Cr (VI) removal are shown in Fig. 7. The results indicated that removal efficiency raised as the adsorbent dosage increased, since plenty of active sites were available for metal ions to be transferred onto the adsorbent surface. However, an opposite trend for Cr (VI) uptake was observed when adsorbent dosage augmented because all accessible vacant sites could not be saturated due to the partial accumulation of adsorbent particles [61]. Based on the revealed results and negligible change in Cr (VI) removal, 3 g/L was selected as an optimum adsorbent dosage.

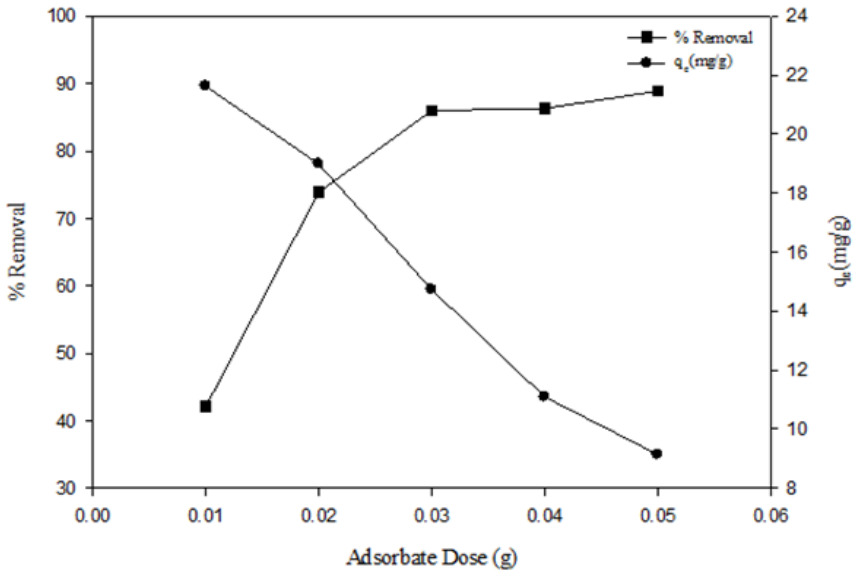

Figure 7. Effect of adsorbent dosage on Cr (VI) removal and adsorption capacity (T=298 K, C_0=51 mg/L, pH of 5).

3.3.3. Effect of contact time and initial concentration on Cr (VI) adsorption

Fig. 8 shows the effect of contact time and initial concentration on Cr (VI) removal at various initial concentrations (i.e., 9, 60, and 90 mg/L). The adsorption experiments were carried out at 25 ℃, pH of 5.0, and adsorbent dosage of 3 g/L [62-63].

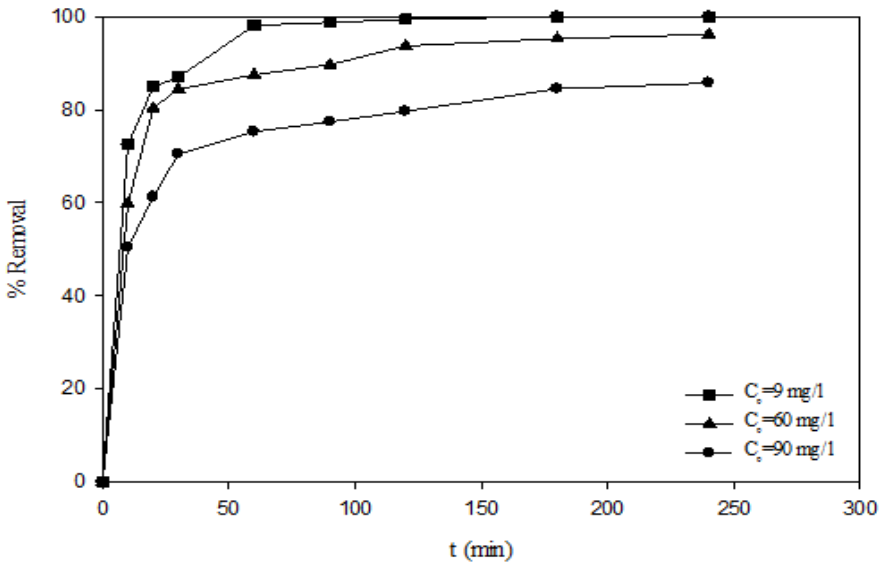

Figure 8. Effect of contact time and initial concentration on Cr (VI) adsorption.

It is evident from Fig. 8 that, for all initial concentrations of Cr (VI) ions, the adsorption process took place promptly at the beginning of the experiment due to the plentifully available adsorption sites in the preliminary stages [63]. In addition, the existence of a strong concentration gradient between bulk solution and adsorbent surface enhances the adsorption rate. However, when the adsorbent became saturated (after 180 min), the adsorption process reached to equilibrium state where Cr (VI) removal efficiency approached 100 %, 96.18 %, and 85.73 %, respectively. It is evident that the required time to get to the equilibrium increases with an increase in the initial concentration of Cr (VI) since, in this step, due to the saturation of exterior site of the adsorbent, diffusion on the interior surfaces occurs at a slow rate.

3.4. Adsorption isotherm

In studying adsorption processes, a useful prospect about the interaction between adsorbates and adsorbent molecules is given by adsorption isotherm models. Also, it provides information about the distribution of adsorbate between the liquid and solid phases at various equilibrium concentrations [64]. In this study, three well-known isotherm models, namely Langmuir, Freundlich, and Langmuir-Freundlich models, were applied to determine the relationship between Cr (VI) ions that were distributed between sorbed and bulk phases.

The Langmuir isotherm model assumes that the adsorption of adsorbate occurs by monolayer uptake on a homogenous surface without any interaction between adsorbed molecules [65]. The non-linear form of the Langmuir isotherm can be expressed as follows:

$$q_e = q_{max}\frac{k_L C_e}{1 + k_L C_e} \quad (3)$$

where q_e is the adsorption capacity at

equilibrium (mg/g), C_e is the Cr (VI) concentration in solution (mg/L) in equilibrium state, q_m denotes the maximal adsorption capacity (mg/g), and k_L is the Langmuir constant and represents the energy of adsorption (L/mg).

Unlike the Langmuir model, the Freundlich isotherm model assumes that the uptake of adsorbate molecules occurs on a heterogeneous adsorbent surface. This model considers that both monolayer and multiple-layer adsorptions can occur during the adsorption process [66]. The non-linear form of the Freundlich isotherm can be expressed as follows:

$$q_e = k_F C_e^{1/n} \quad (4)$$

where 1/n represents the heterogeneity factor of the adsorbent relating to the surface heterogeneity of adsorbent, and k_F is the Freundlich constant (mg/g).

Langmuir-Freundlich isotherm model is a three-parameter model and is a combination of Langmuir and Freundlich models. The non-linear form of the Langmuir-Freundlich isotherm can be expressed as follows:

$$q_e = \frac{q_{max}(k_{LF}C_e)^b}{1 + (k_{LF}C_e)^b} \quad (5)$$

where q_{max} denotes the maximal adsorption capacity (mg/g), k_{LF} is the Langmuir-Freundlich constant, and b represents the heterogeneity factor.

To find the most appropriate model for the Cr (VI) adsorption, equilibrium data at three different temperatures (i.e., 19 ˚C, 25 ˚C, and 35 ˚C) were evaluated by the mentioned models, and the constants related to these models are tabulated in Table 5. Meanwhile, the nonlinear fit of Cr (VI) uptake at the aforementioned temperatures and equilibrium phase is illustrated in Fig. 9. As it is clear from Table 5 and Fig. 9, Langmuir-Freundlich isotherm model had better correlation coefficient than the other models. This implies that, at low concentrations, multilayer adsorption (Freundlich assumption) was dominant and at a higher concentration, monolayer adsorption (Langmuir assumption) occurred, which means that the adsorbent reached its saturation level [61].

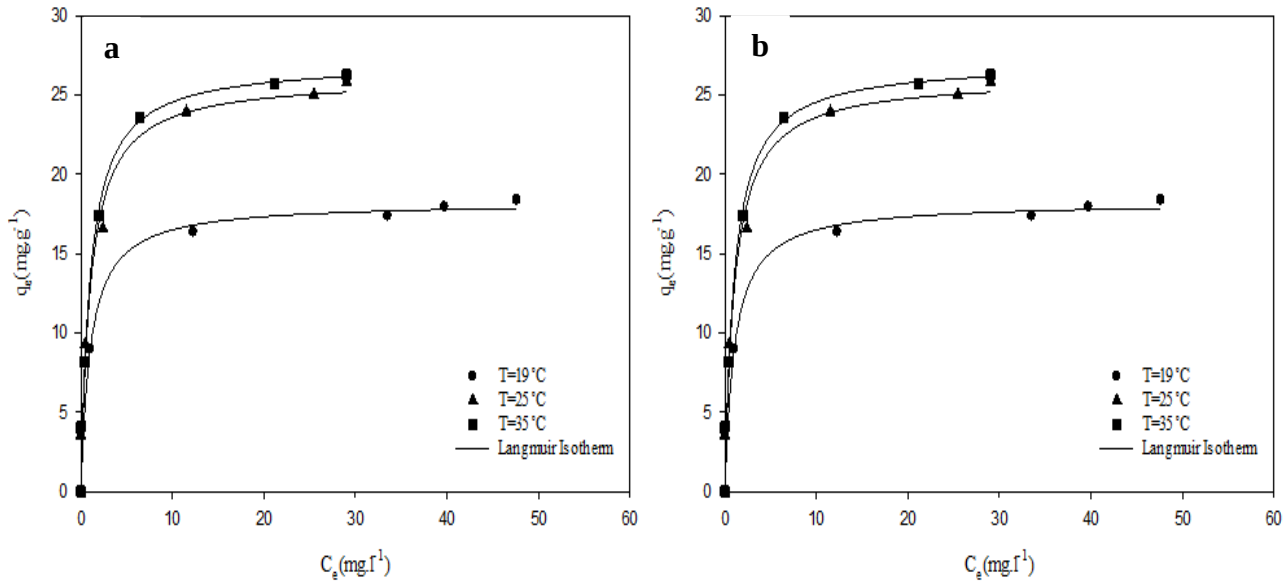

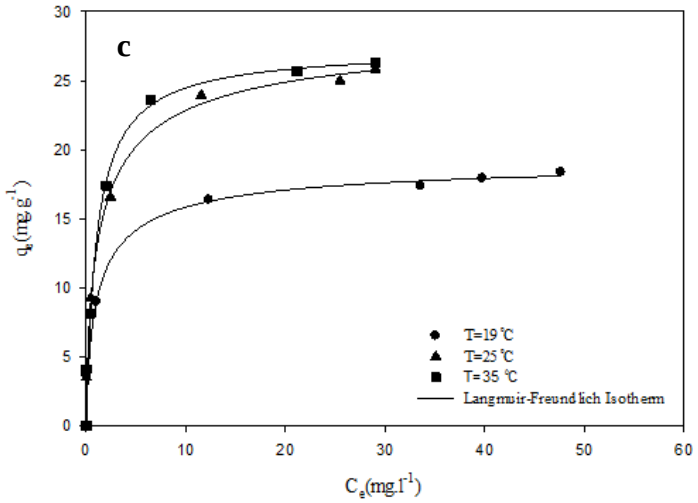

Figure 9. Adsorption isotherm of Cr (VI) on ZIF-67 at three temperatures of 19 ℃, 25 ℃, and 35 ℃: (a) Langmuir isotherm, (b) Freundlich isotherm, and (c) Langmuir- Freundlich isotherm.

Table 5
Isotherm constants for Cr (VI) adsorption on ZIF-67.

T (℃)	Langmuir isotherm			Freundlich isotherm			Langmuir- Freundlich isotherm			
	q_{max} (mg/g)	k_L (l/mg)	R^2	n	k_F (mg/g(l/mg)$^{1/n}$)	R^2	b	q_{max} (mg/g)	k_{LF} (l/mg)	R^2
19	18.2434	0.9471	0.9582	5.8892	9.711	0.9512	0.456	23.2	0.3653	0.9592
25	26.0849	0.9482	0.9747	4.688	12.9681	0.9683	0.7158	26.65	0.9036	0.9808
35	27.0696	0.9787	0.9759	4.796	13.7855	0.9395	0.7459	31.22	0.9341	0.9761

3.5. Adsorption kinetics

Adsorption kinetics can be defined as the quantity of adsorbate that is adsorbed by the adsorbent at a unit of time. Kinetic data provide information about the reaction pathways and mechanism of the reactions which are important for process efficiency [67]. The Cr (VI) ions were found to be adsorbed very rapidly in the initial period of the adsorption process, because of large number of free adsorption sites. Equilibrium was achieved within the first 2 h for initial Cr (VI) concentration of 9 mg/L and within the first 3 h for initial Cr (VI) concentrations of 60 and 90 m/L due to the increasing driving force for mass transfer [68]. Two well-known lumped reaction-based kinetic models, i.e., pseudo-first-order and the pseudo-second-order models were applied to examine the experimental data at different initial concentrations.

The pseudo-first-order equation can be expressed in a nonlinear form as follows:

$$q_t = q_e(1 - e^{-k_1 t}) \quad (6)$$

where q_t is the amount of Cr (VI) adsorbed per unit amount of ZIF-67 at any time t (mg/g), qe is the amount of Cr (VI) adsorbed per unit amount of ZIF-67 in the equilibrium state (mg/g), and k_1 is the rate constant of the pseudo-first order kinetic equation (l/min).

The pseudo-second-order equation can be expressed in a non-linear form as follows:

$$q_t = \frac{k_2 {q_e}^2}{1 + k_2 q_e t} t \quad (7)$$

where q_t is the amount of Cr (VI) adsorbed

per unit amount of ZIF-67 at any time t (mg/g), qe is the amount of Cr (VI) adsorbed per unit amount of ZIF-67 in the equilibrium state (mg/g), and k_2 is the rate constant of the pseudo-second-order sorption (g/mg min). The mechanism may involve sharing of valence forces or through the exchange of electrons between the adsorbent and the adsorbate [63]. All constants and correlation coefficients were determined through non-linear fitting, as listed in Table 6.

In addition, Fig. 10 depicts non-linear fit of the experimental data to gain a better insight into the applicability of kinetic models. According to Table 6, the value of k_2 decreases with increasing the initial concentration, indicating that chemisorption is significant in the rate-limiting step, involving valency forces through sharing or exchange of electrons between Cr (VI) and ZIF-67 [69]. Also, the correlation coefficients (R^2) obtained for the pseudo-second-order kinetic model at all initial concentrations were greater than that for pseudo-first-order kinetic model; therefore, the adsorption of Cr (VI) ions from aqueous solution onto ZIF-67 follows pseudo-second-order kinetic equations.

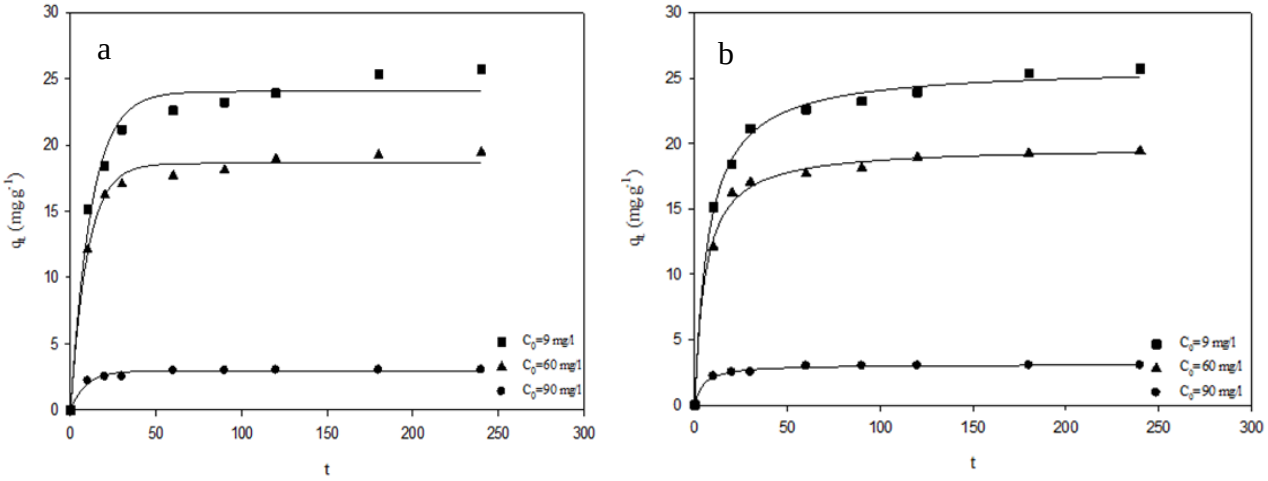

Figure 10. Adsorption Kinetics plots of Cr (VI) adsorption on the ZIF-67: (a) Pseudo first-order kinetic model; (b) Pseudo second-order kinetic model.

Table 6
Kinetic constant parameters obtained for Cr (VI) adsorption on ZIF-67.

C_0 (mg/l)	Pseudo first order				Pseudo-second order			
	$k_1\times10^2$ (l/min)	q_e (mg/g)	$q_{e,exp}$ (mg/g)	R^2	$k_2\times10^2$ (l/min)	q_e (mg/g)	$q_{e,exp}$ (mg/g)	R^2
9	11.47	2.9438	3.028	0.9764	7.0186	3.1046	3.028	0.9945
60	10.14	18.6087	19.4345	0.9911	0.9084	19.7588	19.4345	0.995
90	8.3	24.0334	25.7225	0.9782	0.5161	25.8667	25.7225	0.9962

3.6. Adsorption thermodynamics

The adsorption thermodynamics is investigated to provide insights into the effect of temperature on the adsorption process. Thermodynamic parameters, including the Gibbs free energy ($\Delta G°$), enthalpy ($\Delta H°$), and entropy ($\Delta S°$), are the actual indicators for practical application and are determined using the following equations:

$$\ln K_{eq} = -\frac{\Delta H°}{RT} + \frac{\Delta S°}{R} \quad (8)$$

$$K_{eq} = \frac{C_{ads}}{C_e} = \frac{C_0 - C_e}{C_e} \quad (9)$$

$$\Delta G° = -RT \ln K_{eq} \quad (10)$$

where K_{eq}, C_{ads}, C_e, R, and T are the equilibrium constant, the amount of adsorbate adsorbed on the adsorbent (mol/L), the equilibrium concentration of adsorbate in the solution (mol/L), the gas constant (8.31 4 J/mol K), and the absolute temperature (K), respectively. The values of ΔH^o and $\Delta S°$ can be calculated from the slopes and intercepts of Van't Hoff plot (Eq. 8), and all extracted constants are summarized in Table 7.

According to Table 7, $\Delta H°$ is found to be positive, which indicates the thermophilic nature of the reaction. The positive value of $\Delta S°$ demonstrates the increased randomness at the solid/solution interface during the adsorption process. The negative values of $\Delta G°$ indicate that the adsorption process is spontaneous and feasible in nature. Moreover, the values of $\Delta G°$ decrease with the increasing temperature, revealing that the adsorption of Cr (VI) onto the ZIF-67 is more favorable at higher temperatures. It is worth mentioning that the high value of enthalpy change (i.e., +86.96 kJ/mol) indicated that the sorption process occurred chemically.

Table 7
Thermodynamic parameters for Cr (VI) adsorption on ZIF-67.

T (K)	K_{eq}	$-\Delta G^\circ$ (kJ mol^{-1})	ΔS° (J mol^{-1}K^{-1})	ΔH° (kJ mol^{-1})
292	1.5536	1.69	303.58	86.96
298	6.2316	3.51		
308	10.9621	6.54		

3.7. Desorption studies

Recovery of the adsorbent after the adsorption process and retaining its adsorption capacity after the regeneration is a very important feature for the practical applications. In this study, adsorption-desorption of Cr (VI) was implemented through four sequential cycles. After each cycle of adsorption, ethanol was used as a stripping agent for 3 h. The amount of Cr (VI) uptake in each cycle is illustrated in Fig. 11. The results showed that, after the first cycle, ZIF-67 still exhibited a comparable uptake capacity, proving that the ethanol-washing was an effective technique to remove Cr (VI) from the ZIF-67 structure. This trend declined after three adsorption-desorption cycles, and removal efficiency of ZIF-67 decreased from 94.76 % to 57.7 % due to the reduction of active sites of the adsorbent surface [8].

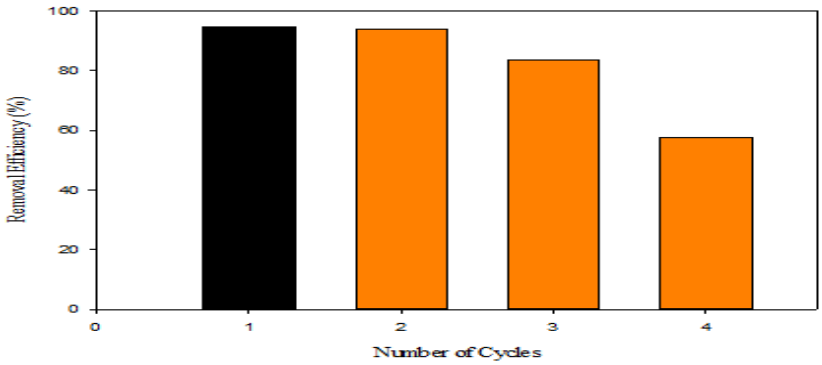

Figure 11. Regeneration of ZIF-67 after Cr (VI) adsorption using ethanol.

4. Conclusions

In the present study, ZIF-67 was synthesized through the solvothermal route and was used to remove Cr (VI) ions from aqueous solution. To maximize the adsorption capacity of ZIF-67, synthesis conditions (i.e., solvent: metal ion molar ratio, ligand: metal ion molar ratio, and synthesis temperature) were optimized. In this regard, solvent: metal ion molar ratio of 4.6, ligand: metal ion molar ratio of 318, and synthesis temperature of 23 ℃ were chosen as the optimum points. The optimum ZIF-67 was characterized through different analyses, and it possessed a high BET surface area of 1767.6 m^2/g with a total pore volume of 0.6885 cm^3/g. The effect of some influential factors, such as pH, adsorbent dosage, initial concentration, and contact time, on adsorption process efficiency was investigated. The results showed that in pH of 5, the adsorbent dosage of 3 g/l and temperature of the optimized ZIF-67 at 19 ℃ had the maximum uptake of 26.27 mg/g for an initial concentration of 107.82 mg/l. Langmuir-Freundlich isotherm model provided a better fit for equilibrium data than other models did. Meanwhile, the adsorption kinetics data followed the pseudo-second-order model with a high correlation coefficient. From a thermodynamic point of view, adsorption of Cr (VI) on ZIF-67 took place spontaneously and endothermically in nature. To assess the durability of ZIF-67, the adsorption-desorption experiment was carried out in three cyclic stages, revealing that ZIF-67 could keep its adsorption capacity untill two sequential cycles.

References

[1] Kano, N., Tanabe, K., Pang, M., Deng, Y. and Imaizumi, H., "Biosorption of chromium from aqueous solution using chitosan", *J. Chem. Chem. Eng.*, **8**, 1049 (2014).

[2] Dai, J., Ren, F. and Tao, C., "Adsorption of Cr (VI) and speciation of Cr (VI) and Cr (III) in aqueous solutions using chemically modified chitosan", *International Journal of Environmental Research and Public Health*, **9** (5), 1757 (2012).

[3] Arenas, L. T., Lima, E. C., dos Santos, A. A., Vaghetti, J. C., Costa, T. M. and Benvenutti, E. V., "Use of statistical design of experiments to evaluate the sorption capacity of 1, 4-diazoniabicycle [2.2. 2] octane/silica chloride for Cr (VI) adsorption", *Colloids and Surfaces, A: Physicochemical and Engineering Aspects*, **297** (1), 240 (2007).

[4] Khedr, S., Shouman, M., Fathy, N. and Attia, A., "Effect of physical and chemical activation on the removal of hexavalent chromium ions using palm tree branches", *ISRN Environmental Chemistry*, (2014).

[5] Chen, J., Hong, X., Zhao, Y. and Zhang, Q., "Removal of hexavalent chromium from aqueous solution using exfoliated polyaniline/montmorillonite composite", *Water Science and Technology*, **70** (4), 678 (2014).

[6] Khosravi, R., Fazlzadehdavil, M., Barikbin, B. and Taghizadeh, A. A., "Removal of hexavalent chromium from aqueous solution by granular and powdered Peganum Harmala", *Applied Surface Science*, **292**, 670 (2014).

[7] Teng, H., Xu, S., Zhao, C., Lv, F. and Liu, H., "Removal of hexavalent chromium from aqueous solutions by sodium dodecyl sulfate stabilized nano zero-valent iron: A kinetics, equilibrium, thermodynamics study", *Separation*

Science and Technology, **48** (11), 1729 (2013).

[8] Li, X., Gao, X., Ai, L. and Jiang, J., "Mechanistic insight into the interaction and adsorption of Cr (VI) with zeolitic imidazolate framework-67 microcrystals from aqueous solution", *Chemical Engineering Journal*, **274**, 238 (2015).

[9] Gheju, M. and Balcu, I., "Removal of chromium from Cr (VI) polluted wastewaters by reduction with scrap iron and subsequent precipitation of resulted cations", *Journal of Hazardous Materials*, **196**, 131 (2011).

[10] Zhao, S., Chen, Z., Shen, J., Qu, Y., Wang, B. and Wang, X., "Enhanced Cr (VI) removal based on reduction-coagulation-precipitation by $NaBH_4$ combined with fly ash leachate as a catalyst", *Chemical Engineering Journal*, **322**, 646 (2017).

[11] Mamais, D., Noutsopoulos, C., Kavallari, I., Nyktari, E., Kaldis, A., Panousi, E., Nikitopoulos, G., Antoniou, K. and Nasioka, M., "Biological groundwater treatment for chromium removal at low hexavalent chromium concentrations", *Chemosphere*, **152**, 238 (2016).

[12] Yang, R., Aubrecht, K. B., Ma, H., Wang, R., Grubbs, R. B., Hsiao, B. S. and Chu, B., "Thiol-modified cellulose nanofibrous composite membranes for chromium (VI) and lead (II) adsorption", *Polymer*, **55** (5), 1167 (2014).

[13] Zhang, Y., Yu, L., Wu, D., Huang, L., Zhou, P., Quan, X. and Chen, G., "Dependency of simultaneous Cr (VI), Cu (II) and Cd (II) reduction on the cathodes of microbial electrolysis cells self-driven by microbial fuel cells", *Journal of Power Sources*, **273**, 1103-1113 (2015).

[14] Rafati, L., Mahvi, A., Asgari, A. and Hosseini, S., "Removal of chromium (VI) from aqueous solutions using Lewatit FO36 nano ion exchange resin", *International Journal of Environmental Science & Technology*, **7** (1), 147 (2010).

[15] Vaiopoulou, E. and Gikas, P., "Effects of chromium on activated sludge and on the performance of wastewater treatment plants: A review", *Water Research*, **46** (3), 549 (2012).

[16] Uysal, M. and Ar, I., "Removal of Cr (VI) from industrial wastewaters by adsorption, Part I: Determination of optimum conditions", *Journal of Hazardous Materials*, **149** (2), 482 (2007).

[17] Rowsell, J. L., Spencer, E. C., Eckert, J., Howard, J. A. and Yaghi, O. M., "Gas adsorption sites in a large-pore metal-organic framework", *Science*, **309** (5739), 1350 (2005).

[18] Haque, E., Jun, J. W. and Jhung, S. H., "Adsorptive removal of methyl orange and methylene blue from aqueous solution with a metal-organic framework material, iron terephthalate (MOF-235)", *Journal of Hazardous Materials*, **185** (1), 507 (2011).

[19] Yang, D. -A., Cho, H. -Y., Kim, J., Yang, S. –T. and Ahn, W. –S., "CO_2 capture and conversion using Mg-MOF-74 prepared by a sonochemical method", *Energy & Environmental Science*, **5** (4), 6465 (2012).

[20] Kim, J., Kim, S. –N., Jang, H. –G., Seo, G. and Ahn, W. –S., "CO_2 cycloaddition of styrene oxide over MOF catalysts", *Applied Catalysis, A: General*, **453**, 175 (2013).

[21] Rocha, J., Carlos, L. D., Paz, F. A. A. and Ananias, D., "Luminescent

multifunctional lanthanides-based metal-organic frameworks", *Chemical Society Reviews*, **40** (2), 926 (2011).

[22] Achmann, S., Hagen, G., Kita, J., Malkowsky, I. M., Kiener, C. and Moos, R., "Metal-organic frameworks for sensing applications in the gas phase", *Sensors*, **9** (3), 1574 (2009).

[23] Humphrey, S. M. and Wood, P. T., "Multiple areas of magnetic bistability in the topological ferrimagnet $[Co_3(NC_5H_3(CO_2)_2\text{-}2,5)_2(\mu_3\text{-}OH)_2(OH_2)_2]$", *Journal of the American Chemical Society*, **126** (41), 13236 (2004).

[24] Horcajada, P., Chalati, T., Serre, C., Gillet, B., Sebrie, C., Baati, T., Eubank, J. F., Heurtaux, D., Clayette, P. and Kreuz, C., "Porous metal-organic-framework nanoscale carriers as a potential platform for drug delivery and imaging", *Nature Materials*, **9** (2), 172 (2010).

[25] Bakhtiari, N. and Azizian, S., "Adsorption of copper ion from aqueous solution by nanoporous MOF-5: A kinetic and equilibrium study", *Journal of Molecular Liquids*, **206**, 114 (2015).

[26] Bertke, J. A., "Synthesis and characterization of coordination polymers and studies for carbon dioxide capture", University of Notre Dame, (2012).

[27] Rowsell, J. L. and Yaghi, O. M., "Metal-organic frameworks: A new class of porous materials", *Microporous and Mesoporous Materials*, **73** (1), 3 (2004).

[28] McKinstry, C., Cathcart, R. J., Cussen, E. J., Fletcher, A. J., Patwardhan, S. V. and Sefcik, J., "Scalable continuous solvothermal synthesis of metal organic framework (MOF-5) crystals", *Chemical Engineering Journal*, **285**, 718 (2016).

[29] Qian, J., Sun, F. and Qin, L., "Hydrothermal synthesis of zeolitic imidazolate framework-67 (ZIF-67) nanocrystals", *Materials Letters*, **82**, 220 (2012).

[30] Liu, Y., Hu, J., Li, Y., Shang, Y. T., Wang, J. Q., Zhang, Y. and Wang, Z. L., "Microwave assisted synthesis of metal-organic framework MIL-101 nanocrystals as sorbent and pseudostationary phase in capillary electrophoresis for the separation of anthraquinones in environmental water samples", *Electrophoresis*, (2017).

[31] Son, W. –J., Kim, J., Kim, J. and Ahn, W. –S., "Sonochemical synthesis of MOF-5", *Chemical Communications*, **47**, 6336 (2008).

[32] Pirzadeh, K., Ghoreyshi, A. A., Rahimnejad, M. and Mohammadi, M., "Electrochemical synthesis, characterization and application of a microstructure $Cu_3(BTC)_2$ metal organic framework for CO_2 and CH_4 separation", *Korean Journal of Chemical Engineering*, 1 (2018).

[33] Yang, H., Orefuwa, S. and Goudy, A., "Study of mechanochemical synthesis in the formation of the metal-organic framework $Cu_3(BTC)_2$ for hydrogen storage", *Microporous and Mesoporous Materials*, **143** (1), 37 (2011).

[34] Lee, J., Farha, O. K., Roberts, J., Scheidt, K. A., Nguyen, S. T. and Hupp, J. T., "Metal-organic framework materials as catalysts", *Chemical Society Reviews*, **38** (5), 1450 (2009).

[35] Moggach, S. A., Bennett, T. D. and Cheetham, A. K., "The Effect of Pressure on ZIF-8: Increasing pore size with pressure and the formation of a high-pressure phase at 1.47 GPa",

Angewandte Chemie, **121** (38), 7221 (2009).

[36] Fairen-Jimenez, D., Moggach, S., Wharmby, M., Wright, P., Parsons, S. and Duren, T., "Opening the gate: Framework flexibility in ZIF-8 explored by experiments and simulations", *Journal of the American Chemical Society*, **133** (23), 8900 (2011).

[37] Park, K. S., Ni, Z., Côté, A. P., Choi, J. Y., Huang, R., Uribe-Romo, F. J., Chae, H. K., O'Keeffe, M. and Yaghi, O. M., "Exceptional chemical and thermal stability of zeolitic imidazolate frameworks", Proceedings of *The National Academy of Sciences*, **103** (27), pp. 10186-10191 (2006).

[38] Wang, F., Tan, Y. -X., Yang, H., Zhang, H. -X., Kang, Y. and Zhang, J., "A new approach towards tetrahedral imidazolate frameworks for high and selective CO_2 uptake", *Chemical Communications*, **47** (20), 5828 (2011).

[39] Shahrak, M. N., Ghahramaninezhad, M. and Eydifarash, M., "Zeolitic imidazolate framework-8 for efficient adsorption and removal of Cr (VI) ions from aqueous solution", *Environmental Science and Pollution Research*, **24** (10), 9624 (2017).

[40] Lai, L. S., Yeong, Y. F., Ani, N. C., Lau, K. K. and Shariff, A. M., "Effect of synthesis parameters on the formation of zeolitic imidazolate framework 8 (ZIF-8) nanoparticles for CO_2 adsorption", *Particulate Science and Technology*, **32** (5), 520 (2014).

[41] Özgen, C., "Production and performance evaluation of ZIF-8 based binary and ternary mixed matrix gas separation membranes", Middle East Technical University, (2012).

[42] Venna, S. R., Jasinski, J. B. and Carreon, M. A., "Structural evolution of zeolitic imidazolate framework-8", *Journal of The American Chemical Society*, **132** (51), 18030 (2010).

[43] Cravillon, J., Nayuk, R., Springer, S., Feldhoff, A., Huber, K. and Wiebcke, M., "Controlling zeolitic imidazolate framework nano-and microcrystal formation: Insight into crystal growth by time-resolved in situ static light scattering", *Chemistry of Materials*, **23** (8), 2130 (2011).

[44] Tsai, C. -W. and Langner, E. H., "The effect of synthesis temperature on the particle size of nano-ZIF-8", *Microporous and Mesoporous Materials*, **221**, 8 (2016).

[45] Jiang, Z., Li, Z., Qin, Z., Sun, H., Jiao, X. and Chen, D., "LDH nanocages synthesized with MOF templates and their high performance as supercapacitors", *Nanoscale*, **5** (23), 11770 (2013).

[46] Shao, J., Wan, Z., Liu, H., Zheng, H., Gao, T., Shen, M., Qu, Q. and Zheng, H., "Metal organic frameworks-derived Co_3O_4 hollow dodecahedrons with controllable interiors as outstanding anodes for Li storage", *Journal of Materials Chemistry, A*, **2** (31), 12194 (2014).

[47] Torad, N. L., Hu, M., Kamachi, Y., Takai, K., Imura, M., Naito, M. and Yamauchi, Y., "Facile synthesis of nanoporous carbons with controlled particle sizes by direct carbonization of monodispersed ZIF-8 crystals", *Chemical Communications*, **49** (25), 2521 (2013).

[48] Guo, X., Xing, T., Lou, Y. and Chen, J., "Controlling ZIF-67 crystals formation

through various cobalt sources in aqueous solution", *Journal of Solid State Chemistry*, **235**, 107 (2016).

[49] Shi, Z., Yu, Y., Fu, C., Wang, L. and Li, X., "Water-based synthesis of zeolitic imidazolate framework-8 for CO_2 capture", *RSC Advances*, **7** (46), 29227 (2017).

[50] Yan, X., Komarneni, S., Zhang, Z. and Yan, Z., "Extremely enhanced CO_2 uptake by HKUST-1 metal-organic framework via a simple chemical treatment", *Microporous and Mesoporous Materials*, **183**, 69 (2014).

[51] Khoshhal, S., Ghoreyshi, A. A., Jahanshahi, M. and Mohammadi, M., "Study of the temperature and solvent content effects on the structure of Cu–BTC metal organic framework for hydrogen storage", *RSC Advances*, **5** (31), 24758 (2015).

[52] Biemmi, E., Christian, S., Stock, N. and Bein, T., "High-throughput screening of synthesis parameters in the formation of the metal-organic frameworks MOF-5 and HKUST-1", *Microporous and Mesoporous Materials*, **117** (1-2), 111 (2009).

[53] Xia, W., Zhu, J., Guo, W., An, L., Xia, D. and Zou, R., "Well-defined carbon polyhedrons prepared from nano metal-organic frameworks for oxygen reduction", *Journal of Materials Chemistry, A*, **2** (30), 11606 (2014).

[54] Juan, Y. and Ke-Qiang, Q., "Preparation of activated carbon by chemical activation under vacuum", *Environmental Science & Technology*, **43** (9), 3385 (2009).

[55] Qin, Q., Wang, Q., Fu, D. and Ma, J., "An efficient approach for Pb (II) and Cd (II) removal using manganese dioxide formed in situ", *Chemical Engineering Journal*, **172** (1), 68 (2011).

[56] El-Ashtoukhy, E. -S., Amin, N. K. and Abdelwahab, O., "Removal of lead (II) and copper (II) from aqueous solution using pomegranate peel as a new adsorbent", *Desalination*, **223** (1-3), 162 (2008).

[57] Tandon, R., Crisp, P., Ellis, J. and Baker, R., "Effect of pH on chromium (VI) species in solution", *Talanta*, **31** (3), 227 (1984).

[58] Gorzin, F. and Ghoreyshi, A. A., "Synthesis of a new low-cost activated carbon from activated sludge for the removal of Cr (VI) from aqueous solution: Equilibrium, kinetics, thermodynamics and desorption studies", *Korean Journal of Chemical Engineering*, **30** (8), 1594 (2013).

[59] Zhao, N., Wei, N., Li, J., Qiao, Z., Cui, J. and He, F., "Surface properties of chemically modified activated carbons for adsorption rate of Cr (VI)", *Chemical Engineering Journal*, **115** (1), 133 (2005).

[60] Giri, A. K., Patel, R. and Mandal, S., "Removal of Cr (VI) from aqueous solution by Eichhornia crassipes root biomass-derived activated carbon", *Chemical Engineering Journal*, **185**, 71 (2012).

[61] Pirzadeh, K. and Ghoreyshi, A. A., "Phenol removal from aqueous phase by adsorption on activated carbon prepared from paper mill sludge", *Desalination and Water Treatment*, **52** (34-36), 6505 (2014).

[62] Al-Othman, Z. A., Ali, R. and Naushad, M., "Hexavalent chromium removal from aqueous medium by activated carbon prepared from peanut shell:

Adsorption kinetics, equilibrium and thermodynamic studies", *Chemical Engineering Journal*, **184**, 238 (2012).

[63] Yadav, S., Srivastava, V., Banerjee, S., Weng, C. -H. and Sharma, Y. C., "Adsorption characteristics of modified sand for the removal of hexavalent chromium ions from aqueous solutions: Kinetic, thermodynamic and equilibrium studies", *Catena*, **100**, 120 (2013).

[64] Jung, C., Heo, J., Han, J., Her, N., Lee, S. -J., Oh, J., Ryu, J. and Yoon, Y., "Hexavalent chromium removal by various adsorbents: Powdered activated carbon, chitosan, and single/multi-walled carbon nanotubes", *Separation and Purification Technology*, **106**, 63 (2013).

[65] Deng, H., Yang, L., Tao, G. and Dai, J., "Preparation and characterization of activated carbon from cotton stalk by microwave assisted chemical activation: Application in methylene blue adsorption from aqueous solution", *Journal of Hazardous Materials*, **166** (2), 1514 (2009).

[66] Lin, K. -Y. A. and Chang, H. -A., "Ultra-high adsorption capacity of zeolitic imidazole framework-67 (ZIF-67) for removal of malachite green from water", *Chemosphere*, **139**, 624 (2015).

[67] Maleki, A., Hayati, B., Naghizadeh, M. and Joo, S. W., "Adsorption of hexavalent chromium by metal organic frameworks from aqueous solution", *Journal of Industrial and Engineering Chemistry*, **28**, 211 (2015).

[68] Debnath, S. and Ghosh, U. C., "Kinetics, isotherm and thermodynamics for Cr (III) and Cr (VI) adsorption from aqueous solutions by crystalline hydrous titanium oxide", *The Journal of Chemical Thermodynamics*, **40** (1), 67 (2008).

[69] Huo, S. -H. and Yan, X. -P., "Metal-organic framework MIL-100 (Fe) for the adsorption of malachite green from aqueous solution", *Journal of Materials Chemistry*, **22** (15), 7449 (2012).